11-1-2006

Magnetopolaron Effect on Shallow Donors in GaN

A. Wysmolek

R. Stepniewski

M. Potemski

B. Chwalisz-Pietka

K. Pakula

See next page for additional authors

Magnetopolaron effect on shallow donors in GaN

A. Wysmołek,[1] R. Stępniewski,[1] M. Potemski,[2] B. Chwalisz-Piętka,[1] K. Pakuła,[1] J. M. Baranowski,[1] D. C. Look,[3,4] S. S. Park,[5] and K. Y. Lee[5]

[1]*Institute of Experimental Physics, Warsaw University, Hoża 69, 00-681 Warsaw, Poland*

[2]*Grenoble High Magnetic Fields Laboratory, CNRS & MPI, BP166X, F-38042 Grenoble Cedex 9, France*

[3]*Semiconductor Research Center, Wright State University, Dayton, Ohio 45433, USA*

[4]*Materials and Manufacturing Directorate, Air Force Research Laboratory, Wright-Patterson Air Force Base, Ohio 45433, USA*

[5]*Samsung Advance Institute of Technology, P.O. Box 111, Suwon, Korea*

(Received 24 May 2006; revised manuscript received 22 September 2006; published 17 November 2006)

Resonant interaction between longitudinal-optic (LO) phonons and electrons bound on shallow donors in GaN is studied using magnetoluminescence of neutral-donor bound excitons (D^0X). The experiments were performed on high-quality freestanding GaN material and heteroepitaxial GaN layers grown on sapphire. In addition to the principal recombination channel of D^0X, in which donors are left in their ground states, two-electron satellites (TES) involving different excited donor excitations, as well as replicas of the principal D^0X transition due to LO phonons, were observed for the oxygen and silicon donors. In order to separate transitions involving ground and excited D^0X states, variable-temperature experiments were performed. The application of high magnetic fields allows tuning of the donor excitations into resonance with the LO phonon energy. This results in a strong enhancement of TES intensity and the appearance of several anticrossing processes in the vicinity of a LO phonon replica of the principal D^0X transition. The observed behavior is explained in terms of a resonant interaction between LO phonons and donor-bound electrons (magnetopolaron effect). The experimental data are described using a phenomenological model that combines the theory of a hydrogen atom in a magnetic field with a model which includes the effects of nonparabolicity, nonresonant polaron corrections, and the resonant magnetopolaron effect on electrons bound to donors. It was found that the interaction in the resonant magnetopolaron regime is stronger for the oxygen than for the silicon donor.

DOI: 10.1103/PhysRevB.74.195205 PACS number(s): 78.55.Cr, 78.20.Ls, 71.38.−k, 71.35.Gg

I. INTRODUCTION

The interaction between electrons and longitudinal-optic (LO) phonons in polar semiconductors has attracted a lot of interest in the past. The great importance of this interaction comes from the fact that it modifies the electron (hole) effective mass.[1,2] The consequences of the electron-phonon interaction are particularly apparent when the electronic excitation energy reaches the LO phonon energy. When such conditions are realized using high magnetic fields, a characteristic anticrossing behavior called the resonant magnetopolaron effect can be observed.[3,4] The splitting of the donor states resulting from the resonant interaction with the LO phonon provides a direct measure of the electron-phonon interaction.[5–7] That is why the resonant magnetopolaron effect has been widely studied in bulk semiconductors[3,4,8,9] as well as in low-dimensional systems including quantum wells[10,11] and quantum dots.[12,13] In the classical far-infrared experiments the intradonor $1s$-$2p_{+1}$ transition energy[10,14] or cyclotron frequency[11] has been tuned by means of a high magnetic field into resonance with the LO phonon energy. In the case of GaN, due to the large effective electron mass and the high LO phonon energy, the observation of a magnetopolaron effect on the $1s$-$2p_{+1}$ intradonor transition is difficult, since it requires very high magnetic fields (around 200 T). A much more realistic task is to study the resonant interaction between the LO phonon and transitions to higher excited donor states.

Recently we have shown that such an idea can be realized in GaN using magnetospectroscopy of neutral donor bound excitons (D^0X).[15] Photoluminescence (PL) of high-quality GaN shows a very rich spectrum involving different electronic and lattice excitations (Fig. 1). In the dominant emission channel of D^0X, referred to as the principal or parent transitions, the neutral donor is left in its ground state after exciton recombination. A different recombination process, in which a part of the D^0X energy is utilized to excite the donor electron, manifests itself as a so-called two-electron satellite

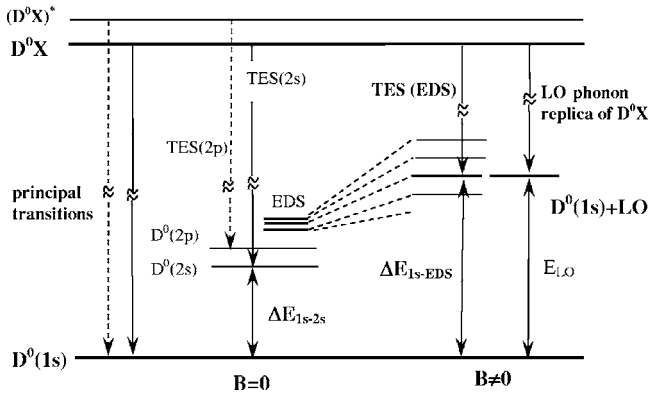

FIG. 1. Potential recombination channels of neutral donor bound excitons involving the D^0X ground state and the first excited state $(D^0X)^*$. For some magnetic fields, the TES emissions involving excited donor states (EDS) coincide in energy with the LO phonon replica of the principal D^0X transition. Here, the energy of the internal donor excitation $\Delta E_{1s\text{-}EDS}$ has been adjusted to the LO phonon energy E_{LO}, a condition required for the observation of the resonant magnetopolaron effect.

(TES). The energy difference between the principal D^0X transition and the corresponding TES is directly related to the intradonor transition energy (e.g., 1*s*-2*s*), and thus provides information about the donor binding energy (Fig. 1). This possibility has generated intensive studies of TES transitions in GaN.[16–22]

Another D^0X recombination process based on excitation in the final recombination state involves a simultaneous emission of a photon and a LO phonon. This process manifests itself in the PL spectrum by the appearance of a replica of the parent transition at an energy lower by a LO phonon energy.

From the point of view of the present work, the most important feature is the simultaneous observation of well-resolved TES transitions involving different excited donor states and a LO phonon replica of the principal D^0X transition.[15] Since intradonor energies depend on a magnetic field, the TES emission can be adjusted to the energy of the LO phonon replica of the principal D^0X transition. In other words, the intradonor excitation energy can be set to the LO phonon energy, which is the required condition for the observation of the resonant magnetopolaron effect (see Fig. 1).

It is worth noting that the present experiment is similar in nature to photoluminescence studies of resonant interactions between shake-up excitations and LO phonons in semiconductor quantum well structures.[23,24] However, to our knowledge this type of experiment has not been reported previously for bulk semiconductors. In this paper detailed experimental studies of the magnetopolaron effect on silicon and oxygen donors in GaN are presented.

The paper is organized as follows. Experimental details are presented in Sec. II. Since recombination processes of neutral donor bound excitons can involve not only different final recombination states but also different initial states, namely, the D^0X ground state and some excited states $(D^0X)^*$, the correct determination of the intradonor excitation energy requires proper identification of the initial and the final recombination states. Thus, before discussing the magnetopolaron effect, a careful analysis of the GaN photoluminescence spectrum is presented. In Secs. III and IV, zero-field characteristics of principal D^0X, TES, and phonon-replica transitions, due to the oxygen and silicon donors, are presented for a freestanding GaN and a selected heteroepitaxial layer. Then magnetic field data involving low-energy excitations (including donor states characterized by the principal quantum number $n \leqslant 3$) are presented and discussed in Sec. V. Section VI is devoted to the magnetic field characteristics of the highly excited donor states and their interactions with the LO phonon. In Sec. VII the experimental results are discussed in terms of a phenomenological model which includes the effects of nonparabolicity, nonresonant polaron corrections, and finally, the resonant magnetopolaron effect for both silicon and oxygen donors. The significant results are summarized in Sec. VIII.

II. EXPERIMENTAL DETAILS

The magnetoluminescence experiments were performed on a thick freestanding GaN sample and a GaN layer grown on sapphire. The freestanding GaN sample was grown by hydride vapor-phase epitaxy (HVPE) on sapphire and then separated from the substrate using a laser lift-off technique at the Samsung Advanced Institute of Technology.[25] Such material shows excellent electrical[26,27] and optical properties.[15,19,27] It has been shown that the main donor centers in freestanding GaN are oxygen and silicon.[19,28] The second sample was a few-μm-thick, Si-doped, GaN layer grown by metal-organic chemical-vapor deposition (MOCVD) on sapphire at Warsaw University. For both samples the *c* axis of the GaN lattice was perpendicular to the surface.

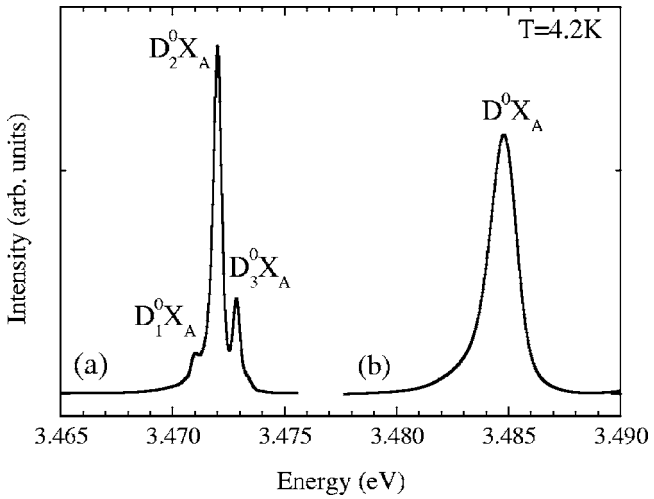

FIG. 2. Principal D^0X_A transitions measured for a freestanding GaN sample (a) and a GaN layer grown on sapphire (b).

Photoluminescence measurements were performed at low temperature (4.2 K) in a magnetic field up to 28 T using an optical-fiber system designed for the ultraviolet. A He-Cd laser operating at 325 nm was used as a source of the PL excitation. The magnetic field *B* was applied along the *c* axis of the GaN lattice ($B \| c$). The spectra were analyzed with a single 0.5 m monochromator equipped with a UV-enhanced charge-coupled device (CCD) camera. The spectral resolution provided by the experimental setup was better than 0.1 meV.

III. ZERO-FIELD CHARACTERISTICS OF PRINCIPAL D^0X TRANSITIONS AND TWO-ELECTRON SATELLITES

In this section, the basic features of the excitonic luminescence are presented. Special attention is given to the identifications of emission lines involving the oxygen and silicon donors in both the freestanding and the heteroepitaxial GaN layers.

Photoluminescence spectra of *n*-type GaN samples are usually dominated by neutral donor bound exciton (D^0X) recombinations. In strain-free homoepitaxial layers the principal D^0X transitions are observed close to 3.472 eV.[29,30] Photoluminescence spectra associated with D^0X recombination are shown in Fig. 2. For the heteroepitaxial layer, a single line (D^0X_A) at an energy 3.4847 eV is assigned to the

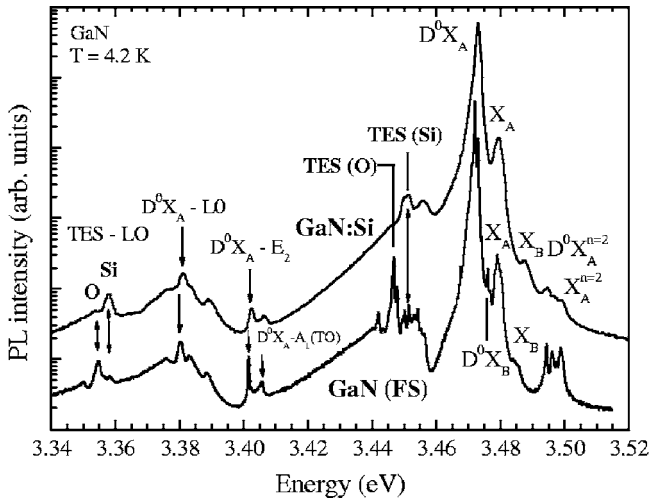

FIG. 3. Photoluminescence spectra of GaN:Si grown by MOCVD on sapphire (upper curve) compared with the emission of the freestanding GaN sample (lower curve). The spectrum of GaN:Si was shifted down in energy by 11.83 meV in order to force the free exciton peak X_A to coincide in the two samples.

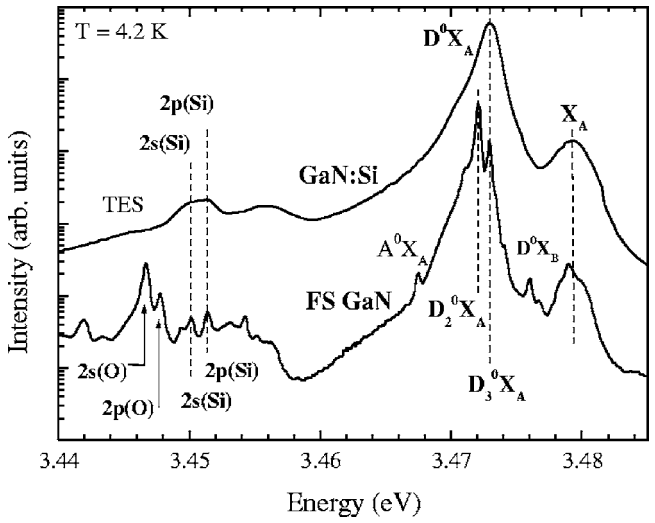

FIG. 4. A comparison of emissions corresponding to the principal and TES transitions in the freestanding GaN sample (lower curve) and the heteroepitaxial GaN:Si layer (upper curve). The spectrum of the heteroepitaxial layer was shifted down so that the free exciton X_A lines coincided in the two samples.

recombination of the exciton originating in the topmost valence subband (A) and bound to the silicon donor. The higher energy here is due to strain, usually present in thin layers grown on sapphire.

For the freestanding sample, three well-resolved lines $D_1^0X_A$, $D_2^0X_A$, $D_3^0X_A$ are found at 3.4710 eV, 3.4720 eV, and 3.4729 eV, respectively.[19] Their energy positions are very close to those observed for neutral donor bound excitons in strain-free homoepitaxial layers.[29,30] Magneto-optical studies[31,32] have shown that all three of these lines split in a similar way, typical for the A exciton bound to a neutral donor in GaN.

The observed energy difference between emissions in the freestanding GaN and heteroepitaxial layer makes direct comparison of the structures due to oxygen and silicon donors difficult. In order to facilitate this task, the PL spectrum of the heteroepitaxial layer was shifted down in energy by 11.83 meV. After such an operation, the energy of the X_A line corresponding to the recombination of the free exciton A is the same in each sample (Figs. 3 and 4). Also, the emissions due to excited states of the free exciton A, labeled as $X_A^{n=2}$, coincide in both spectra. However, the structures due to recombination of the free exciton B (X_B) do not match. This results from the compressive strain present in the heteroepitaxial layer. Among different D^0X transitions observed here, one can distinguish less intense D^0X_B structures involving the free exciton B ground states as well as transitions $D^0X_A^{n=2}$ related to excited states of D^0X_A excitons.[30,18,15]

In the energy range between 3.44 and 3.46 eV, pronounced TES emissions composed of several well-resolved lines are observed. E_2(high) and TO phonon replicas of the principal D^0X transitions are clearly visible at 3.402 eV and 3.406 eV, respectively. In the region around 3.38 eV, the emissions due to the LO phonon replica of principal D^0X_A, D^0X_B transitions and free exciton X_A are observed. The structure shown in Fig. 3 around 3.353 eV corresponds to the LO phonon replica of two-electron satellites.

The correct assignment of a given principal D^0X transition to the corresponding TES structure is a central point for further interpretation of the magneto-optical results. In spite of many efforts, the final elemental identifications of the bound exciton lines in freestanding GaN are still under debate.[20,31] In far infrared spectroscopy (FIR), two dominant donors with binding energies equal to 30.16 meV and 33.2 meV have been identified as Si_{Ga} and O_N, respectively.[33] A consistency between intradonor transition energies provided by FIR spectroscopy and those obtained from the analysis of the two-electron satellites can be obtained by assuming that the $D_2^0X_A$ line involves the oxygen donor, and the $D_3^0X_A$ line, the silicon donor.[20] This assignment is seemingly not in agreement with the results of time-resolved experiments, since the $D_2^0X_A$ line shows a time decay different from that measured for the two-electron satellite corresponding to the oxygen donor.[31] On the other hand, it would be expected that the difference in energy between a particular D^0X line, say that due to Si, and the free exciton line should be independent of the sample. It is thus important to note that the maximum of the D^0X_A emission in the heteroepitaxial layer, which is thought to be connected to Si, coincides with the $D_3^0X_A$ emission line in the freestanding sample. The energy difference between the $D_3^0X_A$ and D^0X_A lines and the free exciton X_A, corresponding to the exciton localization energy on the neutral silicon donor, is about 6.4(2) meV. Simultaneously, the TES lines involving the $2s$ and $2p$ states of the silicon donor, labeled as $2s$(Si) and $2p$(Si) in Fig. 4, also coincide, while the TES lines involving the $2s$ and $2p$ states of the oxygen donor, labeled as $2s$(O) and $2p$(O) in Fig. 4, are observed only in the freestanding sample. It is found that in the case of the silicon donor, the energy distance between the principal transitions and the $2s$(Si) satellite emission is equal to 22.8(1) meV. In the case of the oxygen donor, the distance between the $D_2^0X_A$ line and the $2s$(O) satellite line is 25.5(1) meV.

This observation supports the assignment of $D_3^0X_A$ to silicon, contrary to our previous interpretation, which was based on time-resolved measurements.[19] Consequently, the $D_2^0X_A$ line, which corresponds to the more localized exciton (localization energy of about 7.3(2) meV), can be assigned to the oxygen donor.

Interestingly, the relative intensities of the 2*s* and 2*p* TES transitions are different for the oxygen and silicon donors (Fig. 4). In the case of the oxygen donor, at liquid helium temperature, the 2*s*-TES intensity is stronger than that of the 2*p*-TES, whereas in the silicon case, the opposite is true. Since a similar 2*s*/2*p* intensity ratio is observed for the silicon donor in homoepitaxial GaN layers,[18,30] it can be concluded that the observed 2*s*/2*p* intensity ratios are peculiar to the silicon and oxygen donors themselves rather than to the particular samples chosen for the experiment. The observed difference could be related to the fact that silicon and oxygen occupy different sublattices, which can effectively modify thermalization processes in the initial recombination state of the TES, as will be discussed below.

Supplementary identification of the structures corresponding to the silicon and oxygen donors can be obtained from an analysis of the phonon replicas of the principal transitions. It could be expected that the most intense phonon replica as well as the TES emission should correspond to the dominant donor. Indeed, the emission lines marked in Fig. 3 as D^0X_A-E_2 appear 70.6 meV below the most intense principal transitions, both in the freestanding sample and in the heteroepitaxial layer. This energy distance corresponds very well to the energy of the E_2(high) phonon mode.[34,35] Further phonon replicas, which appear 92.0 meV below $D_2^0X_A$ in the freestanding sample and 92.1 meV below D^0X_A in the heteroepitaxial layer, correspond very well to the A_1(LO) phonon energy measured in bulk GaN by Raman scattering.[34,35]

In short, we conclude that the observed phonon replicas as well as the most intense TES structures observed in the heteroepitaxial layer and in the freestanding sample ($D_2^0X_A$ line) are due to the silicon and oxygen donors, respectively. This is in accordance with the expectation that the dominant donor centers correspond to oxygen in the freestanding sample and silicon in the heteroepitaxial layer.

IV. ZERO-FIELD TEMPERATURE DEPENDENCE OF THE PRINCIPAL TRANSITIONS AND TES LINES

As was mentioned, the assignment of a parent D^0X state to each TES transition is crucial for the calculation of intradonor transitions. In particular, both ground and excited (rotational) D^0X states can be involved. This issue can be clarified on the basis of variable-temperature photoluminescence experiments.

The first experimental evidence of the participation of the rotational excited states of D^0X as initial states in TES transitions was reported by Skromme *et al.*[17] Much closer insight into the energy structure of D^0X in GaN was obtained by means of selective excitation spectroscopy, which reveals several D^0X exited states in the range of a few millielectron volts above the neutral donor bound exciton ground state. The position of the first rotational excited D^0X state was reported to be about 1.3 meV above the ground state.[36]

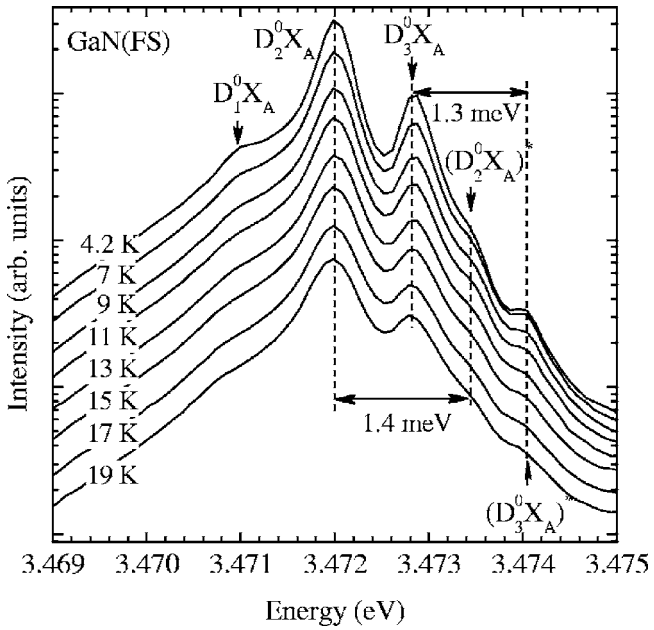

FIG. 5. Emissions due to principal D^0X transitions measured for the freestanding GaN at various temperatures ranging from 4.2 up to 19 K.

Magneto-optical experiments and variable temperature PL studies have shown that the 2*s*-TES transition originates in the ground state of D^0X, whereas the 2*p*-TES originates in the excited state, labeled as $(D^0X)^*$ (see Fig. 1).[19,20]

The observation of principal transitions involving excited states of the neutral donor bound exciton complex is difficult since their intensities are very small as compared to emissions from the D^0X ground state. Nevertheless, a comparison of the temperature dependences of the D^0X and $(D^0X)^*$ lines with the various observed TES lines can facilitate the correlations of the former with the latter. Selected spectra measured for the freestanding sample at different temperatures between 4.2 and 19 K are presented in Fig. 5. It is observed that in addition to the principal transitions originating in the ground states of the neutral donor bound exciton complex ($D_1^0X_A$,$D_2^0X_A$,$D_3^0X_A$), supplementary lines, labeled as $(D_2^0X_A)^*$ and $(D_3^0X_A)^*$, separated from the dominant transitions by about 1.4 and 1.3 meV, respectively, are observed. We attribute them to transitions from the first excited states of neutral donor bound exciton complexes (often designated as I_{2a}^0).[37] For comparison, in Fig. 6, photoluminescence spectra measured for different temperatures in the TES region are presented. It is clearly seen that the intensities of TES lines involving 2*s* donor states decrease in a similar way to the intensities of emissions from the ground states of the D^0X complexes. In the same way, the intensities of TES lines involving 2*p* states show a nonmonotonic temperature behavior similar to that observed for emissions from the excited $(D^0X_A)^*$ states of the donor bound exciton complexes.

In Figs. 7 and 8, the intensity changes of the TES lines of different symmetry are compared with their principal transitions for the silicon and oxygen donors, respectively, in the freestanding sample. The observed temperature behavior is

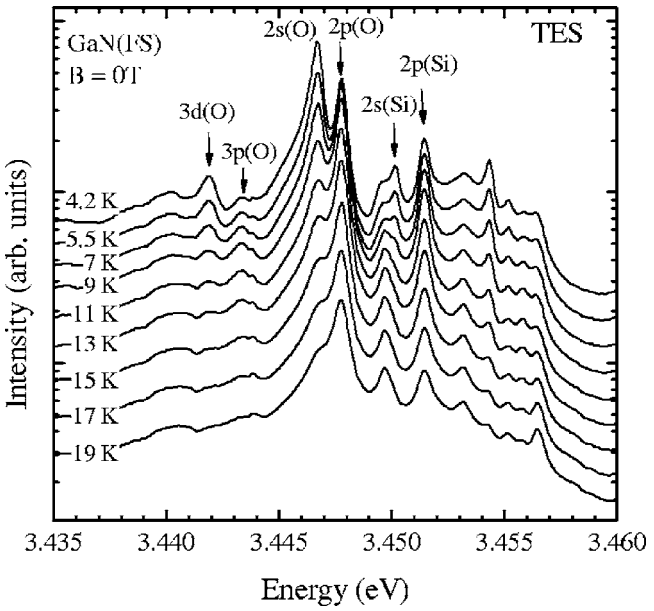

FIG. 6. PL spectra measured at various temperatures ranging from 4.2 up to 19 K for the freestanding GaN in the region of two-electron satellites.

similar for both silicon and oxygen bound excitons. Thermally induced depopulation of the D^0X ground state results in simultaneous intensity decrease of the $D_2^0X_A$ and $D_3^0X_A$ lines and their counterparts in the TES region $2s$(O) and $2s$(Si), respectively. At the same time, the intensities of the TES transitions $2p$(O) and $2p$(Si), originating in the $(D_2^0X_A)^*$ and $(D_3^0X_A)^*$ excited states, respectively, first gain intensity, reaching a maximum at around 8–10 K, and then decrease as a function of temperature.

In summary, the analysis of thermally induced changes in the intensity of principal D^0X_A and corresponding TES transitions enables identification of the initial recombination state of the particular photoluminescence structures. Interestingly, the TES transitions involving $2s$ and $3d$ donor states originate in the ground state of the neutral donor bound exciton, whereas those involving $2p$ and $3p$ donor states are initiated from the excited state of the neutral donor bound exciton. As is shown in Sec. VI, this type of analysis is very useful for the identification of the initial recombination state of TES transitions involving donor excitations taking part in the resonant magnetopolaron effect.

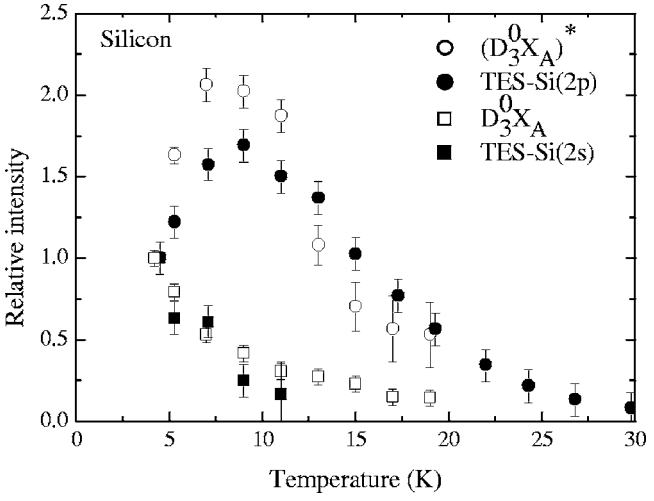

FIG. 7. The temperature dependence of the emission intensity measured in the freestanding GaN for the principal transitions and TES involving $2s$ and $2p$ silicon donor states. Open symbols: squares and circles correspond to principal transitions from the ground and excited states, respectively. Closed symbols correspond to the intensities of TES involving $2p$(Si) (circles) and $2s$(Si) (squares) states, respectively.

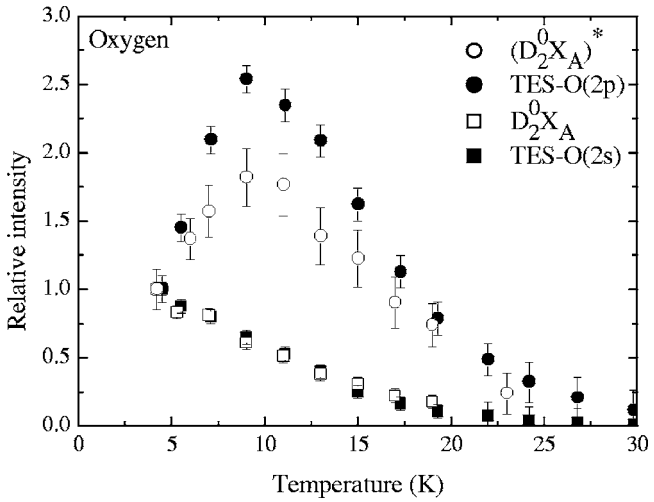

FIG. 8. The temperature dependence of the emission intensity measured in the freestanding GaN for the principal transition involving the ground state of the $D_2^0X_A$ exciton (open symbols) and TES involving $2s$(O) and $2p$(O) oxygen donor states, represented as closed circles and squares, respectively.

V. MAGNETO-OPTICS OF TWO-ELECTRON SATELLITES—LOW-ENERGY EXCITATIONS

In order to discuss the properties of highly excited donor states, the magnetic field behavior of basic TES transitions due to silicon and oxygen donors should be established. Representative PL spectra in the TES region, measured with magnetic field applied parallel to the c axis, are presented in Figs. 9 and 10 for the heteroepitaxial GaN layer and the freestanding sample, respectively. Since in this configuration the electron and hole spin splittings almost cancel each other, the *effective* spin splitting of the D^0X emission is small [g_{eff}=0.64(1)];[38] thus, the splitting patterns observed for the TES transitions are almost directly related to the orbital splittings of the excited donor states. In the energy region presented, the most pronounced effect is observed for $2p$ states.[19] As would be expected, the TES spectrum of the heteroepitaxial layer is dominated by emission corresponding to the silicon donor (Fig. 9). In the case of the freestanding sample, the dominant TES structures are connected with the oxygen donor [$2s$(O), $2p$(O), $3d$(O)]; however, less intense transitions corresponding to the silicon donor [2s(Si), 2p(Si)] are also observed (Fig. 10). It is worth noting that in this sample, in addition to the transitions from the first excited state of the D^0X_A involving the $2p_0$(O) and $2p_0$(Si)

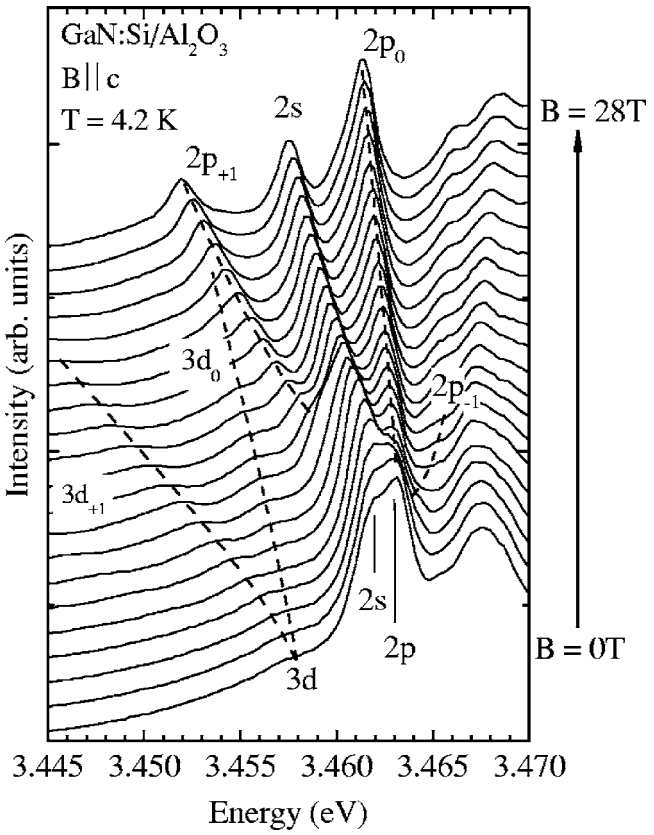

FIG. 9. The two-electron satellites due to silicon donors in the heteroepitaxial layer at 4.2 K for $B\|c$ with B varying from 0 to 28 T.

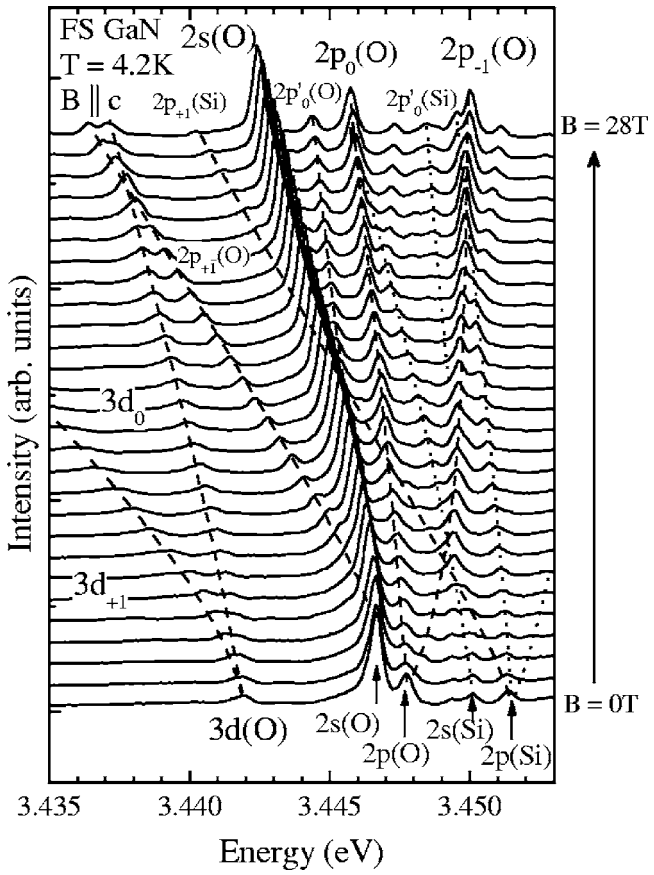

FIG. 10. The two-electron satellites in the freestanding GaN sample measured at 4.2 K for $B\|c$ varying from 0 to 28 T.

states, less intense but still well-resolved transitions, labeled $2p_0'$(O) and $2p_0'$(Si) in Fig. 10, originating in the ground state of the donor bound exciton, are also visible. This observation provides additional information about energy separations between the ground and excited states of the neutral donor bound excitons.

The analysis of the experimental data obtained in a magnetic field allows us to compare the splitting patterns for the transitions attributed to the silicon donor in the heteroepitaxial layer and in the freestanding sample. On the basis of temperature dependences, the observed transitions initiated in the ground D^0X_A state ($2s$, $3d$, etc.) were distinguished from those originating in the excited state of the neutral donor bound exciton complex $[(D^0X_A)^*]$.

The experimental points corresponding to the intradonor silicon transition energies obtained for different magnetic fields for the heteroepitaxial layer and the freestanding sample are presented in Fig. 11. As can be seen, the transition energies are nearly identical, which strongly supports the assertion that silicon donors are indeed present in both samples. The magnetic field evolutions of the intradonor transitions were compared, within the effective mass approximation, with calculations based on the theory of a hydrogen atom in a magnetic field.[39,40]

Since the chemical shift for the silicon donor is too small to be detected in our experiments,[31,20] it was assumed to be zero. The effective mass was assumed to be equal to $m^*=0.215m_0$, which is very close to the value obtained from cyclotron resonance studies.[41] The best fit to the experimental data, including $2s$, $2p$, and $3d$ states, was obtained for an effective Rydberg equal to (30.3 ± 0.1) meV. This result remains in very good agreement with the value 30.2 meV for the silicon donor obtained using FIR spectroscopy.[33] How-

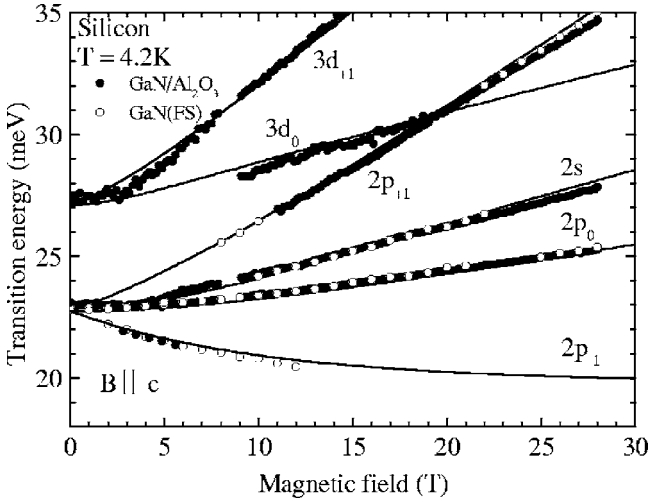

FIG. 11. Magnetic field dependence of intradonor transition energy for selected states of the silicon donor obtained for freestanding GaN (open circles) and for the heteroepitaxial GaN layer (closed circles) grown on sapphire.

ever, the Rydberg determined here is in disagreement with the value of 33.9 meV obtained from the zero-field principle and TES transitions of the oxygen donor, as discussed in Ref. 42.

In order to account for the various magnetic field characteristics of the ground and the first excited state of excitons bound to the silicon donors, a linear correction term, common for all the transitions originating in the excited state of the D^0X_A complex (e.g., $2p$ states), was introduced. The best agreement with the experimental data, measured for silicon donors in the $B\|c$ configuration, was obtained by assuming that $(D^0X_A)^*$, separated by 1.3(1) meV from the neutral donor bound exciton ground state at $B=0$ T, moves up in magnetic field faster than the D^0X_A ground state by 0.019 meV/T. Such an effect was already reported in our previous publication.[19] It is more likely caused by different rotational symmetry[43] than by different effective g-factors of the first excited state $(D^0X)^*$ and the ground state of the D^0X complex; however, this issue needs to be clarified. It is worth noting that the magnetic field behavior of the TES lines could possibly provide valuable information about the excited states of the neutral donor bound exciton complex, which are not easily accessible in the direct magneto-optics of principal transitions. However, such an analysis is beyond the scope of this paper.

The analysis in the case of the oxygen donor, if limited to donor states $n\leqslant 3$, provides an ionization energy of (33.0 ± 0.1) meV (effective Rydberg and chemical shift of 30.3 meV and 2.5 meV, respectively). This finding remains in good agreement with the far-infrared experiments.[28,33] The separation between the ground state and the first excited state of the exciton bound to the neutral oxygen donor was estimated to be about 1.4 meV. It was found that the component of the first excited state $(D_2^0X_A)^*$, which serves as the initial recombination state of the $2p$(O) transition, moves about 0.026 meV/T faster than does the lower spin component of the $D_2^0X_A$ ground state.

The ionization energies obtained for both the silicon and oxygen donor are about 1 meV higher than those reported in our previous publications dealing with freestanding GaN.[19] As was emphasized in Sec. III, this discrepancy results from different assignments of the principal transitions which at that time were based on the time-resolved measurements.[19]

The most important result presented in this section is that the use of the hydrogenic model (including a central cell correction term in the case of the oxygen donor) makes it possible to reasonably describe intradonor transitions up to $n=3$. As it will be shown in the next part, such a method is insufficient to reproduce the magnetic field behavior for excitations with $n>3$, especially for energies near the LO phonon excitation energy.

VI. HIGHLY EXCITED DONOR STATES AND LO PHONONS IN MAGNETIC FIELDS

The magnetic field evolution of the TES spectra involving the donor states $n\geqslant 3$, with magnetic field parallel to the c axis, is shown in Figs. 12 and 13, for the freestanding sample and the heteroepitaxial layer, respectively. It is clearly seen

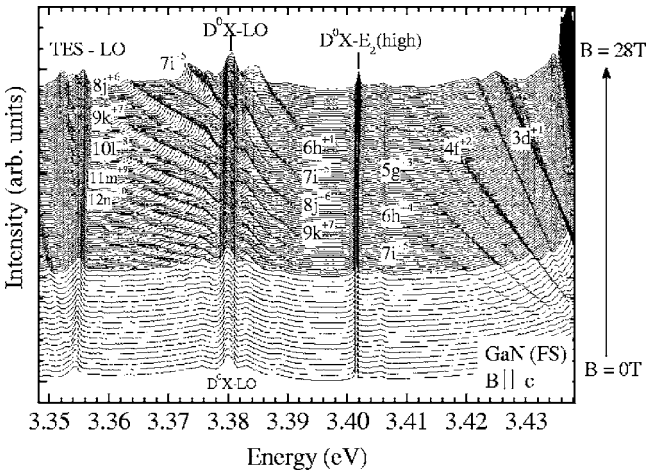

FIG. 12. The two-electron emission, corresponding to the highly excited donor states, measured for the freestanding GaN sample at 4.2 K in a magnetic field $B\|c$ varying from 0 to 28 T.

that in both cases the intensities of the TES lines corresponding to the high-n indexes decrease with increasing magnetic field and disappear completely from the spectrum around the energy of the E_2(high) replica of the principal D^0X transition. However, when the donor excitation energy approaches the LO phonon energy, the intensities of the TES reappear in the emission. The spectra measured for the freestanding GaN (Fig. 12) show several strongly enhanced TES lines passing through the LO phonon replica of the principal D^0X transition. In spite of the fact that in the heteroepitaxial layer the observed lines are broader, several TES lines due to highly excited donor states around the LO phonon replica are clearly observed (Fig. 13). This is the first indication of the resonant interaction between two crystal excitations appearing in the final state of the D^0X recombination: the internal donor excitation and the LO phonon. The second indication of the resonant interaction is a clear anticrossing behavior apparent for several TES lines passing LO phonon replica (Figs. 12 and 13).

However, in both samples, the two-electron satellites are obscured by the background emission corresponding to the

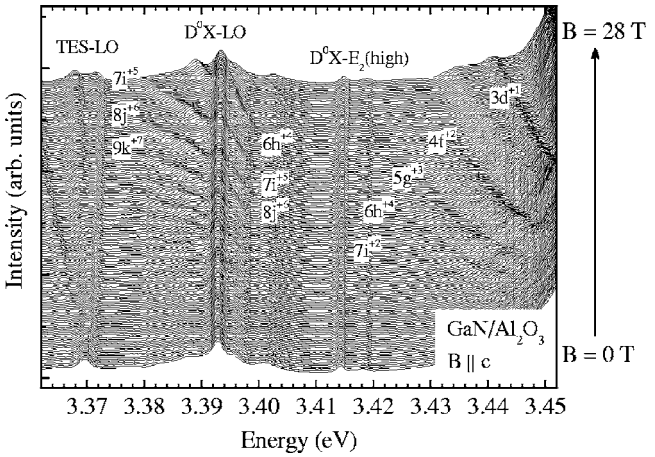

FIG. 13. The two-electron emission, corresponding to the highly excited donor states, measured for the heteroepitaxial GaN layer at 4.2 K in a magnetic field $B\|c$ varying from 0 to 28 T.

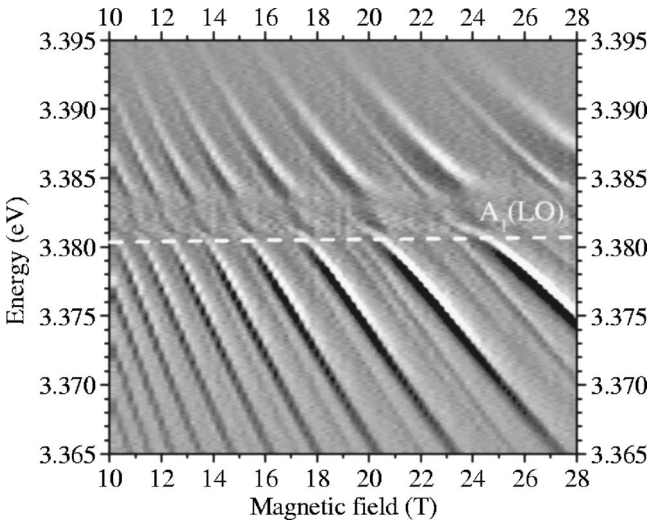

FIG. 14. The spectrally resolved image obtained by subtraction of subsequent PL spectra measured for the freestanding sample with 0.2 T steps. In addition to the dominant transitions clearly showing anticrossing behavior in the region of the LO phonon replica of the principal transition, some less intense transitions are also observed. For these states the interaction with the LO phonons seems to be weaker.

LO phonon replica of the principal D^0X_A transition as well as other excitonic lines. This causes difficulties in the determination of the actual energy positions and intensities of the TES lines in the interaction region. In order to overcome this problem, the spectral changes with each magnetic field step of 0.2 T were analyzed in the vicinity of the LO phonon replica. Such a differential procedure enhances signals that depend strongly on the magnetic field and suppresses features that change slowly with the magnetic field. The result of such a procedure is presented in a form of spectrally resolved images in Figs. 14 and 15 for the oxygen and silicon donors, respectively. In this type of presentation, the actual transition energy is represented by the borders between the white and gray areas of the map. It was verified that the TES energies obtained using such a method reproduce very well those obtained from the raw PL spectrum.

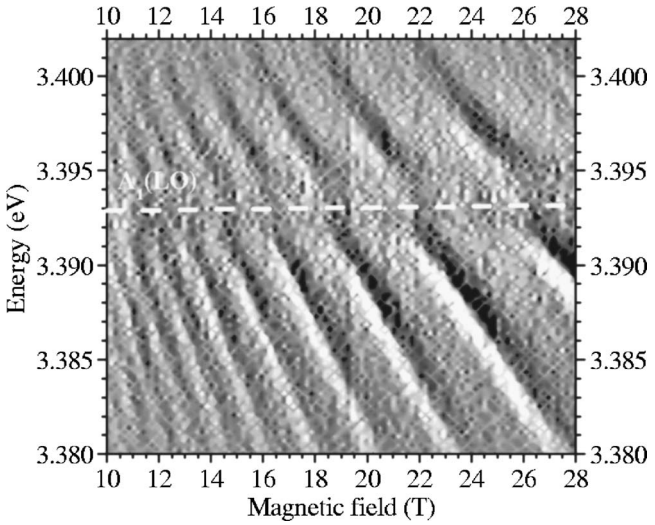

FIG. 15. The spectrally resolved image obtained by subtraction of subsequent PL spectra measured with 0.2 T steps for the heteroepitaxial GaN layer.

As would be expected, the spectrally resolved image obtained for the freestanding sample (Fig. 14) is much better defined than that obtained for the heteroepitaxial layer. In the first case, beside the dominant transitions that we attribute to the oxygen donor, several less intense lines are also resolved. At the moment it is difficult to exclude the possibility that some of them are due to silicon. Surprisingly, two-electron satellites, observed in the freestanding sample, disappear abruptly at an energy of about 3.383 eV and then reappear smoothly in the spectrum at around 3.381 meV, just above the A_1(LO) phonon replica located 92.0 meV below that of the $D_2^0X_A$ transition. This behavior forms a kind of forbidden gap for TES lines in the emission spectrum. Despite the fact that this behavior is not fully understood, it is clearly seen that the TES features taking part in the resonant interaction smoothly cross the energy of the A_1(LO) phonon replica of the principal transition. This indicates that the lattice excitation participating in the interaction with the highly excited donor states has a smaller energy than that of the A_1(LO) phonon mode at the Brillouin zone center.

The emission pattern observed for the heteroepitaxial layer is much less resolved; nevertheless, even here the anticrossing behavior is clearly visible. In this case, the position of the A_1(LO) phonon replica, located 92.1 meV below the principal D^0X transition, seems to fall closer to the center of the gap forbidden for two-electron satellites.

From the point of view of further analysis it is important to identify whether the TES lines observed in the region of interaction with the LO phonon originate from the ground or excited state of the D^0X complex. This information can be obtained from the temperature dependence of the emission in the range of LO phonon replica. The magnetic field evolution of the emission measured up to 14 T for the freestanding sample at $T=4.2$ K and $T=14.5$ K is shown in Fig. 16. It is observed that the TES spectra involved in the interaction with the LO phonon excitation, clearly present in the emission at $T=4.2$ K, are hardly observable in the spectrum at $T=14.5$ K. This indicates that the TES lines participating in the resonant interaction with the LO phonons are connected with the ground state of the D^0X_A complex, which becomes depopulated at elevated temperature.

This observation is confirmed by variable-temperature experiments performed at constant field. Photoluminescence spectra measured at $B=14$ T for several temperatures in the range between 4.2 and 15 K are presented in Fig. 17.

In contrast to the emission corresponding to the LO phonon replica of the free exciton (X_A-LO), the intensities of TES lines due to excited states decrease with rising temperature faster than the intensity of the LO phonon replica of the principal D^0X transition. This behavior confirms that the two-electron satellites involved in the interaction with the LO phonon originate from the ground state of the D^0X_A complex. Thus, in the case of the oxygen donor in the freestanding sample, correct intradonor excitation energies involved in the resonant magnetopolaron effect can be obtained by calculating the energy distance with respect to the $D_2^0X_A$ line,

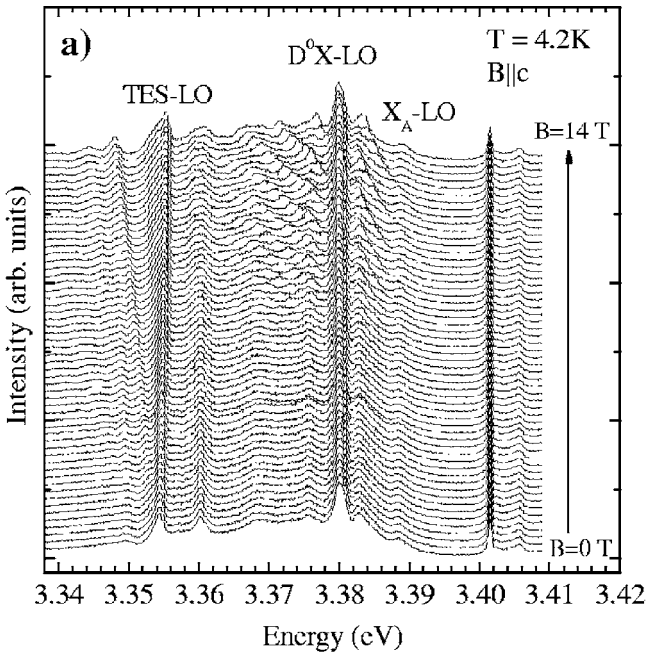

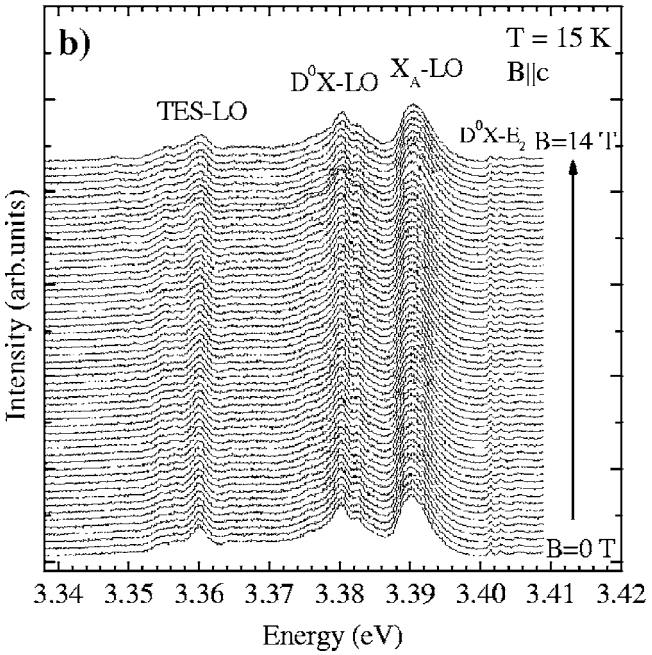

FIG. 16. Magnetic field evolution of the emission in the region of the LO phonon replica of the principal D^0X transition in the freestanding sample measured at (a) 4.2 K and (b) 14.5 K for magnetic fields in the range between 0 and 14 T, applied parallel to the c axis. The transitions due to excited donor states observed at (a) 4.2 K are hardly observable at (b) 14.5 K.

corresponding to the ground state of the exciton bound to the neutral oxygen donor. Similarly, in the case of the heteroepitaxial layer, the silicon donor excitations taking part in the resonant interactions are calculated with respect to the energy of the D^0X line.

The experimental data presented in this section allow tracing the intradonor transition energies for the silicon and oxygen donors in a wide energy range. The magnetic field dependences obtained for the most intense TES lines associated

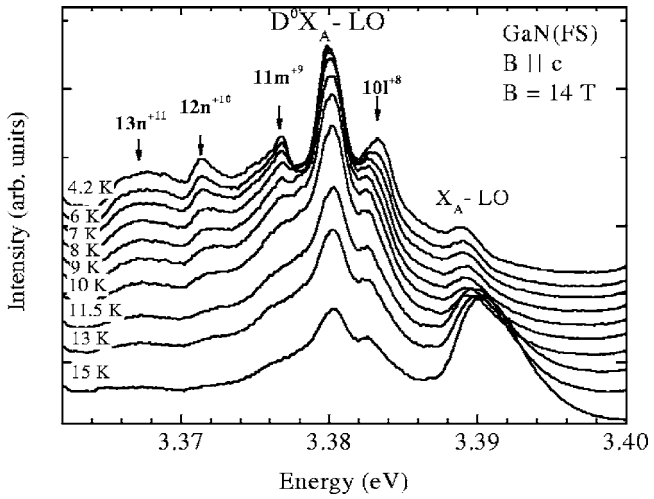

FIG. 17. Temperature evolution of the emission in the region of the LO phonon replica of the D^0X measured for $B=14$ T in the $B\|c$ configuration. The energies of the TES lines due to several excited donor states are marked by arrows.

with the oxygen and silicon donors are summarized in Figs. 18 and 19, respectively.

Detailed analysis of the data involving the magnetic field dependences of the intradonor transition energies is presented in the next section.

VII. DISCUSSION

A complete description of the magnetic field behavior of highly excited donor states in the presence of the electron-

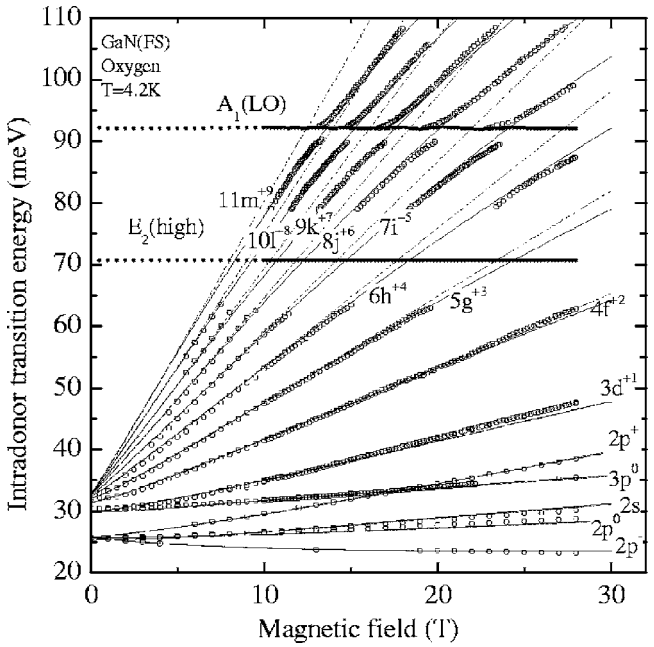

FIG. 18. Excitation energies of the oxygen donor obtained from the photoluminescence experiments (symbols) compared with calculations of the donor states in a magnetic field without (dashed lines) and with (solid lines) nonresonant magnetopolaron corrections.

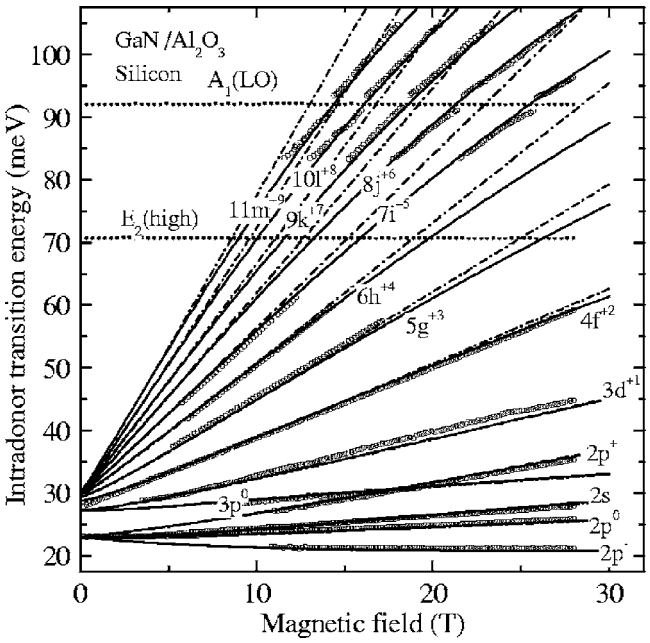

FIG. 19. Excitation energies of the silicon donor obtained from the photoluminescence experiments (symbols) compared with calculations of the donor states in a magnetic field without (dashed lines) and with (solid lines) nonresonant magnetopolaron corrections.

phonon interaction is not readily available. That is why the experimental results are described using a phenomenological model that combines calculations of the hydrogen atomic states in a magnetic field with some analytical solutions obtained for the free electron gas in a magnetic field.

This task is divided into three regimes: (a) Low-energy excitations for which a simple rescaling of the hydrogen model is sufficient to obtain a very good description of the magnetic field behavior; (b) excitation energies above about 40 meV, for which corrections due to the polaron effect, later called "nonresonant" magnetopolaron effects, provide an excellent description of the experimental data, except in the region of the LO phonon energy; and (c) the excitation range close to the LO phonon energy for which the resonant magnetopolaron effect takes place and is approximated by a two-level model.

For the low energy excitations, including 1*s*-2*p* and 1s-2*s* transitions, the observed behavior in a magnetic field up to 28 T can be successfully described by a theory describing hydrogen atomic levels in a magnetic field, based on the effective mass approximation.[39,40] As was shown in Sec. V, it is sufficient to substitute the free electron mass with the effective mass and introduce the effective Rydberg parameter to obtain a reasonable description of the silicon donor. In the case of the oxygen donor, this approximation has to be modified by introducing a chemical shift correction of the 1*s* and 2*s* energies (details—see below).

For excitations beyond 40 meV the situation becomes more complicated. Since the calculation of Ref. 40 provides the magnetic field evolution only for donor states up to $n=4$, the fit to the higher states ($n=5-8$) has been performed according to calculations done by Rosner[44] and Turbiner *et al.*[45] For the higher states, a crude approximation was adopted, namely, that for $n>8$ the energy difference between subsequent states is equal to the cyclotron energy.

Since the experimentally observed excitation energies are high, nonparabolicity effects could be expected to be important for a proper description of the highly excited donor states. The corrections to donor excitation energy E_{ex} arising from nonparabolicity were calculated using the standard Kane model,

$$E_{ex}=\frac{E_g}{2}[-1+[1+4E_p/E_g]^{1/2}], \tag{1}$$

where E_p is the uncorrected donor level energy and E_g is the band gap energy, assumed to be 3.504 eV.[46]

The results of the calculations based on the hydrogen-like model, including correction for nonparabolicity, are presented as broken lines in Figs. 18 and 19. It is clearly seen that this model very well describes excitations below 50 meV but does not account properly for the observed bending of the magnetic field dependences of the intradonor excitation energies for highly excited donor states ($n>3$). Consequently, the theoretical curves obtained in such a way do not cross the LO phonon energy in the magnetic field values observed experimentally. This indicates that the simplest hydrogen-like model, corrected for nonparabolicity, is not sufficient to serve as a basis for the further analysis of the resonant magnetopolaron effect.

Our theoretical description can be improved by taking into account the influence of the electron-phonon interaction. We include in our model the nonresonant part of this interaction based on the results obtained by Peeters and Devreese for Landau levels of the free electron gas subjected to magnetic fields.[5]

It is convenient that Ref. 5 provides an analytical expression for the inclusion of the electron-phonon self-energy for the *N*th Landau level in the low-magnetic-field limit, defined by the relation $\hbar\omega_c \ll E_{\mathrm{LO}}$, where $\hbar\omega_c$ is the cyclotron energy. This limiting approximation appears to be applicable in our case, since even in magnetic fields as high as 28 T, the cyclotron energy in GaN is much smaller than the LO phonon energy ($\hbar\omega_c \approx 0.15\ E_{\mathrm{LO}}$).

In order to account for the enhanced electron-phonon interaction, due to the fact that we are dealing with localized electron states, an additional fitting parameter p was introduced to the original formula presented in Ref. 5. After such a modification, the magnetic-field-induced correction to the donor state energy pinned below the *N*th Landau level takes the form

$$\Delta E_N = -\alpha\left[1+\frac{2N+1}{12}\frac{\hbar\omega_c}{E_{\mathrm{LO}}}\right]E_{\mathrm{LO}} + \\ -\alpha p\left[\frac{18N^2+18N-1}{240}\left(\frac{\hbar\omega_c}{E_{\mathrm{LO}}}\right)^2 + \frac{90N^3+135N^2-37N-6}{2016}\left(\frac{\hbar\omega_c}{E_{\mathrm{LO}}}\right)^3\right]E_{\mathrm{LO}}, \tag{2}$$

where α is the Fröhlich constant and p is the fitting parameter.

The first term of the above expression is equivalent to a shift of the energy scale by a value $\Delta E = -\alpha E_{\mathrm{LO}}$ and replacement of the bare electron effective mass m_b by the polaron mass

$$m^* = \frac{m_b}{(1 - \alpha/6)}.$$

This modification can be easily incorporated into the hydrogen-like model of the donor states in magnetic fields. The second part of Eq. (2) is especially important for the donor states pinned below Landau levels with high N indices. It was assumed that donor states with the same magnetic number $m > 0$, belonging to the same family pinned below certain Landau levels $N = m$, experience the same energy shift due to nonresonant magnetopolaron corrections. However, even for states with $m = +1$ ($2p^{+1}$ and $3d^{+1}$), the influence of this correction is noticeable, and comparing with the previous approximation, has to be compensated by a small reduction of the effective mass.

The best fit to the experimental data was obtained with the parameter p equal to 2.3(1) and 2.2(1) for the oxygen and silicon donor, respectively. The value of the Fröhlich constant $\alpha = 0.44$ was taken from Ref. 47. The bare effective mass of $m_b = 0.195$ was found to provide the best description of the experimental data in the wide energy range. However, it would be worth noting that the splitting between $2p^{-1}$ and $2p^{+1}$ states, which corresponds to the cyclotron resonance energy, is better described when using the bare mass value corresponding to the polaron mass $m^* = 0.222 m_0$ obtained in the far-infrared studies.[41]

The resulting theoretical curves are presented in Figs. 18 and 19. The donor states obtained by this process pass centrally between split-off branches resulting from the resonant interaction with the LO phonon.

Before discussion of the resonant effects, let us focus on the identification of states giving rise to the dominant TES transitions observed around the LO phonon replica. Surprisingly, the best fit to the experimental data was found for the series of states including $3d^{+1}, 4f^{+2}, 5^{g+3}, 6h^{+4}, \ldots n^{l^m}$, for which the principle quantum number n, the orbital momentum l, and magnetic quantum number m, satisfy the relations $l = n - 1$, and $m = n - 2$. The mechanism making these particular states dominant among other TES states is not clear, and this issue needs to be clarified both theoretically and experimentally.

The fitting procedure applied here, covering a wide energy range, provides a consistent picture of the binding energies of the silicon and oxygen donors. Since for the silicon donor no chemical shift was assumed, its binding energy corresponds directly to the effective Rydberg in GaN, which is 30.28(5) meV. This value is in very good agreement with the binding energies calculated on the basis of the $1s$-$2p$ transitions measured in the far-infrared experiments.[33,41] However, it disagrees with the zero-field analysis of the main D^0X oxygen line and the associated $n = 2$, 3, and 4 TES lines, which seem to indicate that oxygen is a hydrogenic donor with a binding energy of 33.9 meV, which then is also the effective Rydberg.[42] The origin of this disagreement is not known at this time but may involve different interpretations of some of the various lines.

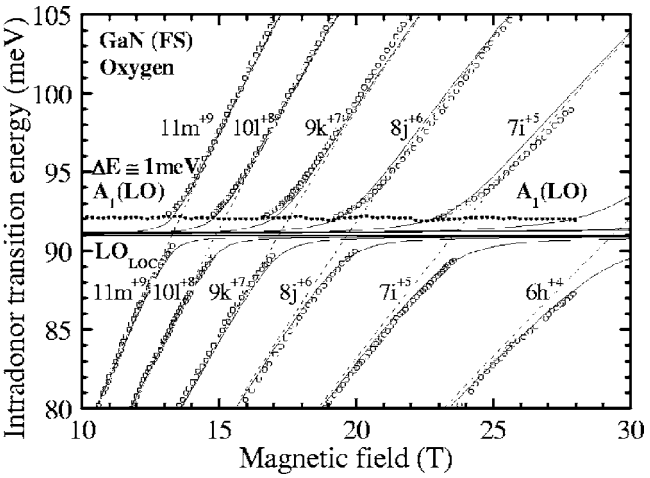

FIG. 20. Excitation energies of the oxygen donor in the range of the resonant interaction with the LO phonon. The experimental data represented by symbols are compared with calculations (lines) based on the model described in the text.

From the fitting procedure, the zero-field separation between the ground state and the first excited state of the exciton bound to the silicon donor was found to be $\Delta E_p = 1.3(1)$ meV. The correction to the magnetic field behavior of the first excited state of the exciton bound to the neutral silicon donor was determined as 0.019 meV/T.

The calculations made for the oxygen donor were performed under the assumption that the chemical shift of the $2s$ state is equal to 1/8 of the chemical shift for the $1s$ state. This approximation results directly from the hydrogen model, in which the wave-function density at the center (donor core) changes for the ns states as $1/n^3$.

The best fit to the oxygen donor excitations was obtained for a chemical shift of 2.7(1) meV, which corresponds to a binding energy of 33.0(1) meV. The zero-field separation between the ground and the first excited state of the exciton bound to the oxygen donor was found to be $\Delta E_p = 1.4(1)$ meV. The correction to the magnetic field behavior of the first excited state, with respect to the ground state, of the neutral exciton bound to the oxygen donor was found to be 0.027(4) meV/T.

Within experimental accuracy, these donor binding energies are consistent with those achieved from the analysis presented in Sec. V.

A good description of the highly excited donor states allows us to concentrate now on the resonant magnetopolaron interaction which manifests itself in the vicinity of the LO phonon energy. Experimental points corresponding to the intradonor excitations around the LO phonon energy are shown in Figs. 20 and 21, for the oxygen and silicon donor, respectively. The dashed lines represent the calculated magnetic field dependence of the donor levels, corrected for the nonresonant magnetopolaron effect. They divide the experimental points into two branches: $E_-(B)$ below and $E_+(B)$ above the LO phonon. This behavior can be reproduced using a simple model of two interacting quantum levels,

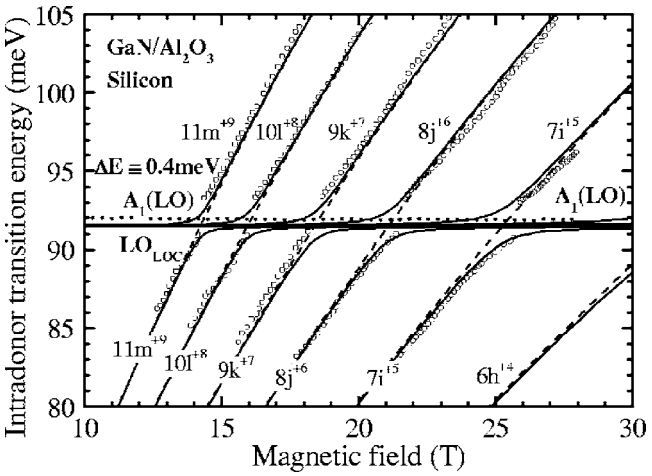

FIG. 21. Excitation energies of the silicon donor in the range of the resonant interaction with the LO phonon. The experimental data represented by symbols are compared with calculations (lines) based on the model described in the text.

$$E_{\pm}(B) = \frac{1}{2}(E_d(B) + E_{\mathrm{LO}} \pm \sqrt{(E_d(B) - E_{\mathrm{LO}})^2 + 4(\Delta_N)^2}), \tag{3}$$

where $E_d(B)$ is the initial donor excitation energy (corrected for the nonresonant effects) corresponding to the magnetic field B, and Δ_N is the interaction parameter assigned to the Nth Landau level.

According to Eq. (3), the splitting between the upper and lower branches, under the condition $E_d(B)=E_{\mathrm{LO}}$, is twice the magnitude of Δ_N. In analogy to the resonant magnetopolaron effect on free carriers, it was assumed that the interaction parameter Δ_N changes with Landau level number according to the formula $\Delta_N=\Delta_1 N^{-2/3}$.[5,6] The results of fitting curves for the oxygen and silicon donor are shown in Figs. 20 and 21, respectively. The good agreement between theoretical curves and experimental points makes possible a meaningful comparison of the resonant magnetopolaron effect on the oxygen and silicon donors.

First of all, it can be concluded that the assumption about the interaction strength, i.e., $\Delta_N=\Delta_1 N^{-2/3}$, seems to work reasonably well. Nevertheless, this dependence is rather weak and thus, complete verification would require experiments at higher magnetic fields, which would allow the observation of the splitting of donor states attached to Landau levels with lower N. The observed magnetopolaron effect for the oxygen donor is found to be stronger than that for the silicon donor. The best fit for the oxygen donor was obtained for a Δ_1 parameter of 4.8(1) meV, whereas for the silicon donor a value of 3.1(1) meV was obtained. Since, according to the applied model, the experimentally observed splitting should be twice Δ_1, it would be expected that the splitting of the $1s$-$2p_{+1}$ transition should be about 9.6 meV for oxygen and 6.2 meV for silicon. These values are of the same order as those observed for the magnetopolaron effect on the $1s$ -$2p_{+1}$ transition in GaAs[10] and CdTe.[14] However, a direct comparison of these results is difficult since the magnetopolaron effect depends not only on the Fröhlich constants and the LO phonon energy, but also on other parameters such as the donor binding energy. This experimental result shows that the magnitude of the resonant magnetopolaron interaction is different for different shallow donor species in the same material. Another difference in the behavior of the oxygen and silicon states manifests itself in the observed reduction of the LO phonon energy involved in the resonant interaction. In the case of the oxygen donor the best fit to the experimental data was obtained for the phonon energy E_{loc} =91.0(1), which is about ΔE=1 meV smaller than the energy observed for the LO phonon replica 92.0(1) meV in the freestanding sample. For the silicon donor, the energy of the active phonon mode provided by the fitting procedure is E_{loc}=91.5(1), as compared to the 92.1(1) meV observed for the LO phonon replica of the principal D^0X_{A} transition in the heteroepitaxial layer. Thus, for the silicon donor the observed "lowering" of the phonon energy (ΔE=0.6 meV) is smaller than in the case of the oxygen donor.

The observed decrease of the active phonon energy with respect to the energy of the A_1(LO) mode at the center of the Brillouin zone would indicate that the interaction involves some local phonon modes or phonons bound to the neutral donor centers. Phonons bound to neutral donors were observed for the first time in n-type GaP.[48] Since that time, phonons bound to donor or acceptor impurities have been studied in different polar semiconductors.[49] In GaP the energies of bound phonons on the S, Sn, and Te donors were found to be between 0.5 and 0.8 meV lower in energy than the energy of the LO phonon at the center of the Brillouin zone.[49] Thus, the energy shift observed in the case of the oxygen donor in GaN, which could be estimated to be on the order of a few tenths of a meV, would be reasonable. However, the idea of bound phonons is usually invoked when the LO phonon energy is smaller than the main intradonor transition energy.[50] Thus, this proposal cannot be directly applied in our case. On the other hand, it would be natural that the interaction of the electron bound on the donor center with the LO phonon should affect both the donor and the lattice excitation. There is no doubt that donor states are modified by the interaction with the lattice; thus, it would be expected that the lattice excitation taking part in the interaction with the donor should be also modified. The stronger the modification of the donor wave function, the bigger the expected effect on the energy of the phonon interaction with the donor. Such a behavior is indeed observed. Another explanation of the observed effects is based on the fact that the localization of the donor wave function increases the volume available in k space for LO phonons involved in the interaction. Since the energy of the A_1(LO) decreases as a function of k vector around the center of the Brillouin zone,[34] the energy of the lattice excitation involved in the magnetopolaron effect could be effectively lowered by a few tenths of a millielectron volt. Because oxygen and silicon donors occupy different sublattices, the coupling of the donor excitations to the lattice vibrations would be different, which in turn could result in the size of the observed effect.

VIII. SUMMARY

Different emission channels due to recombinations of excitons bound to oxygen and silicon donors have been studied

in high quality GaN. A comparison of the luminescence observed in freestanding GaN with that in high quality heteroepitaxial GaN doped with silicon has facilitated the identification of emission structures characteristic of both the silicon and oxygen donors. It has been shown that the energy differences with respect to the free exciton X_A line, for both the principal transitions (bound exciton localization energies) and the two-electron satellites (e.g., corresponding to intradonor transition energies $1s$-$2s$ and $1s$-$2p$), are nearly the same for the silicon donor in the freestanding material as for that in the strained heteroepitaxial layer. This information should be helpful in differentiating silicon- and oxygen-related transitions in the excitonic spectra of GaN.

Special attention has been given to the participation of the excited (rotational) states of the D^0X in the principal transitions and two-electron satellites. Variable-temperature photoluminescence experiments have allowed us to distinguish between recombination processes involving the ground state and the excited states of the neutral donor bound exciton complex. The energy separation between the ground state and the first excited state of the excitons bound to the neutral silicon and oxygen donors has been found to be 1.3(1) meV and 1.4(1) meV, respectively.

The magnetospectroscopy of TES spectral features, performed in magnetic fields up to 28 T, have provided important information concerning the oxygen and silicon donors in GaN. First of all, they have allowed identification of the symmetry of the donor states corresponding to the most intense TES lines. From the fitting procedure, applied over a large energy range, binding energies consistent with earlier FIR data have been obtained. For the silicon donor no chemical shift has been found. A binding energy of 30.28(5) meV has been obtained, and this must correspond to the effective Rydberg in GaN. The best fit to the oxygen donor excitations, including highly excited donor states, has been obtained for a binding energy of 33.0(1) meV and a chemical shift of 2.7(1) meV. These values are consistent with an analysis limited to donor states $n \leqslant 3$.

However, in Ref. 42, an analysis of zero-field spectra for the principle transition and $n=2$, 3, and 4 TES lines of the oxygen donor seems to fit a nearly exact hydrogenic model, with both the binding energy and the Rydberg equal to 33.9 meV. This zero-field model gives about the same binding energies for oxygen and silicon as those deduced from the magnetic-field spectra; however, the chemical shifts are much different, zero for oxygen, and 3.6 meV for silicon.

By applying high magnetic fields, donor excitations could be tuned into resonance with the LO phonon energy. This interaction permitted observation of both resonant and nonresonant magnetopolaron effects on the oxygen and silicon donor. It has been found that the resonant magnetopolaron interaction is more pronounced for the oxygen donor. The estimated splitting of the $1s$-$2p^{+1}$ transition resulting from the resonant magnetopolaron effect is expected to be about 9.6 and 6.2 meV for the oxygen and silicon donors, respectively. The effective energy of the LO phonon modes involved in the resonant interaction have been found to be smaller than the energy of the A_1(LO) phonon mode involved in the replica of the principal transition. As in the case for other parameters related to the magnetopolaron effect, the observed energy lowering is larger for the oxygen donor.

In order to shed more light on the details of the observed effects, more precise experimental data are required. This may require both higher quality in the investigated samples (especially the silicon-doped samples) and also a higher range in the magnetic field available for the experiments. Moreover, the experimental data need to be analyzed with a more general theoretical approach, describing the magnetic field behavior of donor excitations in a polar medium.

ACKNOWLEDGMENTS

This work was partially supported by the European Commission from the 6th Framework Program "Transnational Access-Specific Support Action," Contract No. RITA-CT-2003-505474. The work of D.C.L. was supported by AFOSR Grant F49620-03-1-0197, monitored by G. Witt and K. Reinhardt, and Air Force Contract F33615-00-C-5402, monitored by Jeff Brown. The Grenoble High Magnetic Field Laboratory is associated with the INPG and University Joseph Fourier de Grenoble.

[1] H. Fröhlich, Adv. Phys. **3**, 325 (1954).
[2] R. P. Feynman, Phys. Rev. **97**, 660 (1955).
[3] E. J. Johnson and D. M. Larsen, Phys. Rev. Lett. **16**, 655 (1966).
[4] B. D. McCombe and R. Kaplan, Phys. Rev. Lett. **21**, 756 (1968).
[5] F. M. Peeters and J. T. Devreese, Phys. Rev. B **31**, 3689 (1985).
[6] P. Pfeffer and W. Zawadzki, Solid State Commun. **57**, 847 (1986).
[7] P. Pfeffer, Phys. Rev. B **57**, 12156 (1998), and references therein.
[8] T. Ruf, R. T. Phillips, A. Cantarero, G. Ambrazevicius, M. Cardona, J. Schmitz, and U. Rössler, Phys. Rev. B **39**, 13378 (1989).
[9] V. López, F. Comas, C. Trallero-Giner, T. Ruf, and M. Cardona, Phys. Rev. B **54**, 10502 (1996).
[10] J. P. Cheng, B. D. McCombe, J. M. Shi, F. M. Peeters, and J. T. Devreese, Phys. Rev. B **48**, 7910 (1993).
[11] A. J. L. Poulter, J. Zeman, D. K. Maude, M. Potemski, G. Martinez, A. Riedel, R. Hey, and K. J. Friedland, Phys. Rev. Lett. **86**, 336 (2000).
[12] S. Hameau, Y. Guldner, O. Verzelen, R. Ferreira, G. Bastard, J. Zeman, A. Lemaître, and J. M. Gérard, Phys. Rev. Lett. **83**, 4152 (1999).
[13] S. Hameau, J. N. Isaia, Y. Guldner, E. Deleporte, O. Verzelen, R. Ferreira, G. Bastard, J. Zeman, and J. M. Gérard, Phys. Rev. B **65**, 085316 (2002).
[14] M. Grynberg, S. Huant, G. Martinez, J. Kossut, T. Wojtowicz, G. Karczewski, J. M. Shi, F. M. Peeters, and J. T. Devreese, Phys.

Rev. B **54**, 1467 (1996).
[15] A. Wysmolek, M. Potemski, R. Stępniewski, J. M. Baranowski, D. C. Look, S. K. Lee, and J. Y. Han, Phys. Status Solidi B **235**, 36 (2003).
[16] A. Fiorek, J. M. Baranowski, A. Wysmolek, K. Pakuła, and M. Wojdak, Acta Phys. Pol. A **92**, 742 (1997).
[17] B. J. Skromme, H. Zao, B. Goldenberg, H. S. Kong, M. T. Leonard, G. E. Bulman, C. R. Abernathy, and S. J. Pearton, Mater. Res. Soc. Symp. Proc. **449**, 713 (1997).
[18] A. Wysmolek, V. F. Sapega, T. Ruf, M. Cardona, M. Potemski, P. Wyder, R. Stępniewski, K. Pakuła, J. M. Baranowski, I. Grzegory, and S. Porowski, in *Proceedings of the International Workshop on Nitride Semiconductors 2000*, IPAP Conf. Series No. 1 (IPAP, Tokyo, 2000), p. 579.
[19] A. Wysmolek, K. P. Korona, R. Stępniewski, J. M. Baranowski, J. Błoniarz, M. Potemski, R. L. Jones, D. C. Look, J. Kuhl, S. S. Park, and S. K. Lee, Phys. Rev. B **66**, 245317 (2002).
[20] J. A. Freitas, Jr., W. J. Moore, B. V. Shanabrook, G. C. B. Braga, S. K. Lee, S. S. Park, and J. Y. Han, Phys. Rev. B **66**, 233311 (2002).
[21] Q. Yang, H. Feick, and E. R. Weber, Appl. Phys. Lett. **82**, 3002 (2003).
[22] M. A. Reshchikov, D. Huang, F. Yun, L. He, H. Morkoc, D. C. Reynolds, S. S. Park, and K. Y. Lee, Appl. Phys. Lett. **79**, 3779 (2001).
[23] M. S. Skolnick, D. J. Mowbray, D. M. Whittaker, and R. S. Smith, Phys. Rev. B **47**, 6823 (1993).
[24] L. V. Butov, V. I. Grinev, V. D. Kulakovskii, and T. G. Andersson, Phys. Rev. B **46**, 13627 (1992).
[25] S. S. Park, I.-W. Park, and S. H. Chou, Jpn. J. Appl. Phys., Part 2 **39**, L1141 (2000).
[26] D. C. Look and J. R. Sizelove, Appl. Phys. Lett. **79**, 1133 (2001).
[27] D. C. Reynolds, D. C. Look, B. Jogai, A. W. Saxler, S. S. Park, and J. Y. Han, Appl. Phys. Lett. **77**, 2879 (2000).
[28] W. J. Moore, J. A. Freitas, Jr., G. C. B. Braga, R. J. Molnar, S. K. Lee, K. Y. Lee, and I. J. Song, Appl. Phys. Lett. **79**, 2570 (2001).
[29] K. Pakuła, A. Wysmołek, K. P. Korona, J. M. Baranowski, R. Stępniewski, I. Grzegory, M. Bockowski, J. Jun, S. Krukowski, M. Wroblewski, and S. Porowski, Solid State Commun. **97**, 919 (1996).
[30] K. Kornitzer, T. Ebner, K. Thonke, R. Sauer, C. Kirchner, V. Schwegler, M. Kamp, M. Leszczynski, I. Grzegory, and S. Porowski, Phys. Rev. B **60**, 1471 (1999).
[31] A. Wysmolek, K. P. Korona, R. Stępniewski, J. M. Baranowski, J. Błoniarz, M. Potemski, R. L. Jones, D. C. Look, J. Kuhl, S. S. Park, and S. K. Lee, Phys. Rev. B **69**, 157302 (2004).
[32] R. Stępniewski, A. Wysmolek, and M. Potemski, Phys. Status Solidi A **201**, 181 (2004).
[33] W. J. Moore, J. A. Freitas, Jr., S. K. Lee, S. S. Park, and J. Y. Han, Phys. Rev. B **65**, 081201(R) (2002).
[34] T. Ruf, J. Serrano, M. Cardona, P. Pavone, M. Pabst, M. Krisch, M. D'Astuto, T. Suski, I. Grzegory, and M. Leszczynski, Phys. Rev. Lett. **86**, 906 (2001).
[35] M. S. Liu, L. A. Bursill, S. Prawer, K. W. Nugent, Y. Z. Tong, and G. Y. Zhang, Appl. Phys. Lett. **74**, 3125 (1999).
[36] G. Neu, M. Teisseire, P. Lemasson, H. Lahreche, N. Grandjean, F. Semond, B. Beaumont, I. Grzegory, S. Porowski, and R. Triboulet, Physica B **302-303**, 39 (2001).
[37] C. H. Henry and K. Nassau, Phys. Rev. B **2**, 997 (1970).
[38] A. Wysmolek, M. Potemski, R. Stępniewski, K. Pakuła, J. M. Baranowski, J. Lusakowski, I. Grzegory, S. Porowski, G. Martinez, and P. Wyder, Phys. Status Solidi B **216**, 11 (1999).
[39] Yu. P. Kravchenko, M. A. Liberman, and B. Johansson, Phys. Rev. A **54**, 287 (1996).
[40] P. C. Macado and N. C. McGill, J. Phys. C **19**, 873 (1986).
[41] A. M. Witowski, K. Pakuła, J. M. Baranowski, M. L. Sadowisk, and P. Wyder, Appl. Phys. Lett. **75**, 4154 (1999).
[42] D. C. Look, Z.-Q. Fang, and B. Claflin, J. Cryst. Growth **281**, 143 (2005).
[43] M. P. Silverman, Phys. Rev. A **24**, 342 (1981).
[44] W. Rosner, G. Wunner, H. Herold, and H. Ruder, J. Phys. B **17**, 29 (1984).
[45] A. V. Turbiner, J. Phys. A **17**, 859 (1984).
[46] R. Stępniewski and A. Wysmolek, Acta Phys. Pol. A **90**, 681 (1996).
[47] A. S. Barker, Jr. and M. Ilegems, Phys. Rev. B **7**, 743 (1973).
[48] P. J. Dean, D. D. Manchon, Jr., and J. J. Hopfield, Phys. Rev. Lett. **25**, 1027 (1970).
[49] P. Galtier and G. Martinez, Phys. Rev. B **38**, 10542 (1988), and references therein.
[50] P. Seguy, M. Zigone, and G. Martinez, Phys. Rev. Lett. **68**, 518 (1992), and references therein.